Postprint of: Zmuda M., Szczepański S., Kozieł S., A New Coupler Concept for Contact-less High-Speed Data Transmission Monitoring, IEEE TRANSACTIONS ON INSTRUMENTATION AND MEASUREMENT, Vol. 62, Iss. 2 (2013), pp. 328-334, DOI: 10.1109/TIM.2012.2217666

A New Coupler Concept for Contact-less High Speed Data Transmission Monitoring

M. Zmuda*, S. Szczepański* and S. Kozieł**

*Faculty of Electronics, Telecommunications and Informatics,
Gdańsk University of Technology,
ul. Narutowicza 11/12, 80-233 Gdańsk, Poland

**Engineering Optimization & Modeling Center,
School of Science and Engineering, Reykjavik University,
Menntavegur 1, 101, Reykjavik, Iceland

***Abstract*- This paper presents a new concept of a coupler that can be applied to high speed data transmission contact-less measurements. The proposed approach is dedicated for differential signal transmission monitoring in microstrip coupled lines on PCBs (Printed Circuit Board). The coupler, produced on a separate PCB, is overlayed on the transmission line with the differential signal, and delivers decoupled differential signal to the main measurement path. The main advantage of this solution is that no dedicated connectors are required for the measurement process, which results in product cost reduction and design simplification. The complete design methodology of the proposed coupler has been described. Theoretical considerations have been confirmed by the example coupler prototype that was fabricated and measured. The measurement results show that the proposed concept may be advantageous for contact-less signal monitoring in widely used high speed interconnections realized on cheap FR-4 PCBs.**

***Index Terms*- Differential signal coupler, microstrip coupler, high speed data transmission, digital transmission, measurement**

I. INTRODUCTION

A substantial progress in the development of telecommunication devices has been observed in recent years. Providers supply more and more sophisticated services, such as real time video transmission, broadband internet access or video on demand. These new features require increased transmission bandwidth [9]-[14], which results in the growing demands for the performance of the equipment itself. Modern societies of the developed countries are greedy for technical innovations. The broadband equipment industry will continue to grow rapidly. Under such circuimstances, manufacturing cost of a single device becomes an important factor [15]-[19]. An effective fabrication cost can be reduced in the many ways. Some of them can be introduced through measurement and validation process optimization without compromising quality [20]-[25]. Attempts to solve this problem have been made for a long time, for example, by eliminating the measurement connectors [1], [5]. With a suitable approach, this way can bring additional savings in the production and start-up process.

This paper presents the new concept of a coupler for contact-less high speed data monitoring on PCB, which does not degrade the transmission in the monitored transmission line in the frequency band of interest. The main task of this coupler is to deliver the probed signal to the subsequent components of the measurement system. The main design prerequisities are the following: (i) the coupler must ensure sufficient level of the measured signal decoupling, (ii) it should not degenerate transmission in the main line. Additionally, the coupler should be constructed in such a way that it could be conveniently attached to the circuit under testing. This technology can be used for reducing the cost of the product diagnostic by eliminating dedicated measurement connectors, run-time system debugging or reverse engineering. The main contribution of the paper is a differential signal coupler concept together with the complete design methodology based on well known methods for classical couplers [7], as well as a measurement verification of the device fabricated in several variants. The presented concept, particularly the use of a shifted configuration, the discussion of the design methodology for the proposed coupler with the classical equations for conventional couplers, as well as measurements, constitute the oryginal work of the authors.

The coupler concept, together with the theoretical considerations regarding the relationships between the signals in each element of the circuit, is described in Section II. Section III shows the complete design methodology with all dependencies given analytically. An

example project of the coupler which aims at differential signal monitoring in the existing transmission line (realized on a cheap FR-4 laminate) with measurement results and a dedicated method of the measurement set calibration for all considered variants, is described in section IV. Three different coupler configurations were implemented and analyzed: a coupler fabricated on the same PCB as the transmission line, a coupler fabricated on separate PCB which is then attached to the PCB containing the transmission line under test, and, finally, a coupler whose branches are fabricated on the two separate PCBs. As a reference, to verify that the coupler does not significantly affect the working conditions of the monitored transmission line, all the measurement results are compared to the transmission parameters of the line without the coupler. We conclude the paper in Section V.

II. CONCEPT

The main problem of the high speed transmission monitoring is a proper signal probing without affecting transmission in the monitored line. Contact-less probing can be realized by endowing the PCB with a coupler on the monitored transmission line [1]. In this approach, it is necessary to satisfy a few of conditions. Most importantly, the overlayed coupler should not significantly affect the impedance of the main line - this assumption can be satisfied by using sufficiently small coupling factor and the appropriate structure of coupler's board implementation. On the other hand, the coupling factor must be sufficiently large to decouple a part of the signal which can be subsequently processed in the next functional block of the measurement system in the specified frequency band. We assume that the coupler works with an existing transmission line so that only the geometrical dimensions of the coupler itself are considered to be the designable parameters. A differential signal coupler is composed of the two simple, classical proximity couplers (lines 5-6 and 7-8) located on both sides of the transmission line (1-2, 3-4) as shown on Fig.1.

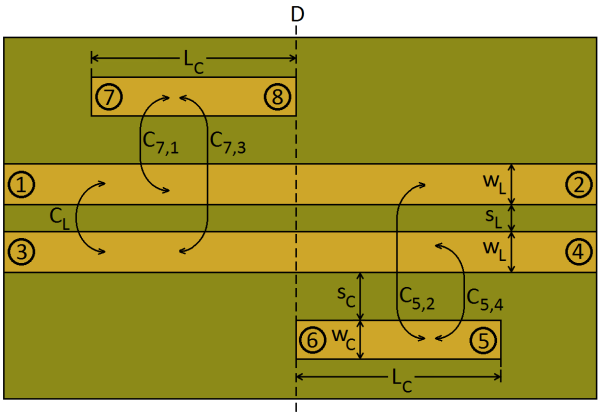

Fig.1 Concept of differential signal coupler

Minimum impact on the transmission line is accomplished by shifting one coupler apart from the other one along the line. This configuration allows us to eliminate the undesired capacitances between branches. Useful signal in the transmission line V_d (defined as difference of signals in lines 1-2 and 3-4) is guided by a pair of parallel, coupled paths (the main transmission line). A total guided signal V_d can be represented as a set of two components defined as signals V_1 and V_3 between a common ground plane and the corresponding wires. Signals V_1 and V_3 have the same amplitudes and opposite phases. In the far field area, the sum of V_1 and V_3 is zero. Let us define the following coupling factors in [dB] for coupling phenomena between next paths: C_L, $C_{5,2}$, $C_{5,4}$, $C_{7,3}$, $C_{7,1}$ (Fig.1). Geometrical relations between the dimensions of the transmission line and the coupling strips allow us to assume that $C_{5,2} < C_{5,4}$ and analogically $C_{7,3} < C_{7,1}$. Let us define an additional signal V_d' (defined as the difference of the signals at points 5 and 7) and assume that $V_d' \sim V_d$. Geometrical dimensions of the coupling lines, s_C, w_C and L_C, are determined by the desired differential coupling factor C_{diff} (defined as a coupling factor between a differential transmission line port 1-3 and a coupler output port 6-7) for a given frequency with minimal coupler impact on the transmission line. We demonstrate that taking into account the aforementioned assumptions allows us to exploit the design methodology adopted from the classical directional coupler [6][7] as a proper tool for designing the coupler overlayed on the transmission line while maintaining a particular structure of the coupler's board.

III. DESIGN

As mentioned in the previous section, the differential signal coupler, in the proposed configuration, can be considered as a pair of two independent single-branch couplers. This assumption allows us to adopt known analytical relations for classical coupler synthesis [6][7] to a differential coupler design. Let us assume that the coupling factors for both branches are equal ($C_{5,4} = C_{7,1} = C_B$). Impedances for even Z_{0e} and odd Z_{0o} modes for the pairs of single coupling branch and single strip of transmission line (line 1-2 and branch 7-8, line 3-4 and branch 5-6) with the assumed characteristic impedance Z_0 can be expressed as follows [7]:

$$Z_{oe} = Z_0 \sqrt{\frac{1 + 10^{(C_B/20)}}{1 - 10^{(C_B/20)}}} \tag{1}$$

$$Z_{oo} = Z_0 \sqrt{\frac{1 - 10^{(C_B/20)}}{1 + 10^{(C_B/20)}}} \tag{2}$$

where C_B is a forward coupling factor between a single coupling branch and a single closer line in [dB].

The distance s_c between the transmission line and the branch of the coupler can be determined using the dependencies below [6]:

$$s_c/h = \frac{2}{\pi} cosh^{-1}(M) \tag{3}$$

$$M = \frac{cosh\left[\frac{\pi}{2}\left(\frac{w_c}{h}\right)'_{so}\right] + cosh\left[\frac{\pi}{2}\left(\frac{w_c}{h}\right)_{se}\right] - 2}{cosh\left[\frac{\pi}{2}\left(\frac{w_c}{h}\right)'_{so}\right] - cosh\left[\frac{\pi}{2}\left(\frac{w_c}{h}\right)_{se}\right]} \tag{4}$$

where h is a PCB substrate height, $(w_c/h)_{se}$ and $(w_c/h)_{so}$ are auxiliary parameters for even and odd modes.

The parameter $(w_c/h)'_{so}$ is expresed as a sum of $(w_c/h)_{so}$ and $(w_c/h)_{se}$ with constant factors. Auxiliary parameters $(w_c/h)_{so}$, $(w_c/h)_{se}$ are calculated by changing auxiliary parameter R to $(Z_{oo}/2)$ for $(w_c/h)_{so}$ and $(Z_{oe}/2)$ for $(w_c/h)_{se}$ in equation:

$$(w_c/h)_{se,so} =$$

$$\frac{8\sqrt{\left[exp\left(\frac{R}{42.4}\sqrt{(\epsilon_r+1)}\right)-1\right]\frac{7+(4/\epsilon_r)}{11}+\frac{1+(1/\epsilon_r)}{0.81}}}{\left[exp\left(\frac{R}{42.4}\sqrt{(\epsilon_r+1)}\right)-1\right]} \tag{5}$$

where ϵ_r is a dielectric constant of substrate.

$$\left(\frac{w}{h}\right)'_{so} = 0.78\left(\frac{w}{h}\right)_{so} + 0.1\left(\frac{w}{h}\right)_{se} \tag{6}$$

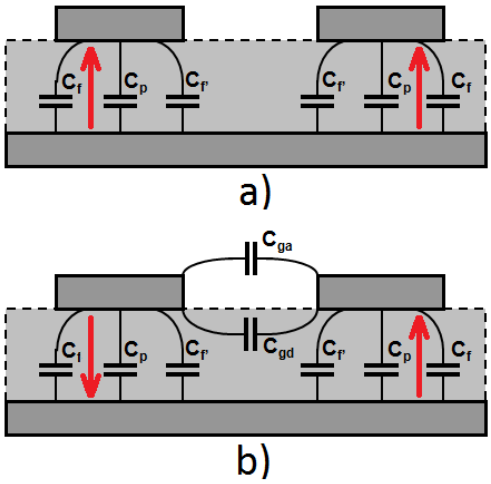

Fig.2 Capacitance distribution in the coupled lines for even (a) and odd (b) mode.

Finally, the w_c/h ratio can be specified as [7]

$$w_c/h = \frac{1}{\pi}cosh^{-1}(d) - \frac{1}{2}\left(\frac{s_c}{h}\right) \tag{7}$$

$$d = \frac{cosh\left[\frac{\pi}{2}\left(\frac{w_c}{h}\right)_{se}\right](g+1)+g-1}{2} \tag{8}$$

$$g = cosh\left[\frac{\pi}{2}\left(\frac{s_c}{h}\right)\right] \tag{9}$$

The length L_C of the coupling branch, which ensures a desired value of the coupling factor at the operating frequency f_0, is equal to a quarter of a wavelength in the substrate, λ, i.e.,

$$L_C = \frac{\lambda}{4} = \frac{c}{4f\sqrt{\epsilon_{eff}}} \tag{10}$$

The total effective dielectric permitivity ϵ_{eff} can be calculated on the basis of an effective permitivity for even ϵ_{effe} and odd ϵ_{effo} modes.

$$\epsilon_{eff} = \left[\frac{\sqrt{\epsilon_{effe}}+\sqrt{\epsilon_{effo}}}{2}\right]^2 \tag{11}$$

These parameters strongly depend on capacitances between the conducting stripes and the ground plane, and the conductive stripes mutually (Fig.2). The way of calculating permitivities for both modes with full capacitance calculations is shown below [7].

$$\epsilon_{effe} = \frac{C_e}{C_{e1}} \tag{12}$$

$$\epsilon_{effo} = \frac{C_o}{C_{o1}} \tag{13}$$

where C_e, C_o are total capacitances for each mode and C_{o1}, C_{e1} are similar capacitances but with air as a substrate. The total capacitance for even mode (Fig.2a) is a sum of these three factors.

$$C_e = C_p + C_f + C'_f \tag{14}$$

$$C_p = \epsilon_0\epsilon_r\frac{w}{h} \tag{15}$$

where ϵ_0 is a dielectric permitivity of vocuum

$$C_f = \frac{\sqrt{\epsilon_{seff}}}{2cZ_0} - \frac{C_p}{2} \tag{16}$$

$$\epsilon_{seff} = \frac{\epsilon_r+1}{2} - \frac{\epsilon_r-1}{2}F(w/h) \tag{17}$$

$$F(w/h) =$$

$$\begin{cases} (1+12h/w)^{-1/2} + 0.041(1-w/h)^2 & \text{for } \left(\frac{w}{h}\right) \leqslant 1 \\ (1+12h/w)^{-1/2} & \text{for } \left(\frac{w}{h}\right) > 1 \end{cases} \tag{18}$$

$$C'_f = \frac{C_f}{1+A(h/s)tanh(\frac{10h}{s})}\left(\frac{\epsilon_r}{\epsilon_{seff}}\right)^{1/4} \tag{19}$$

$$A = exp\left[-0.1exp\left(2.33-1.5\frac{w}{h}\right)\right] \tag{20}$$

Similar considerations can be carried out for the odd mode (Fig.2b). For this case, the inter-strip mutual capacitance must be added.

$$C_o = C_p + C_f + C_{ga} + C_{gd} \tag{21}$$

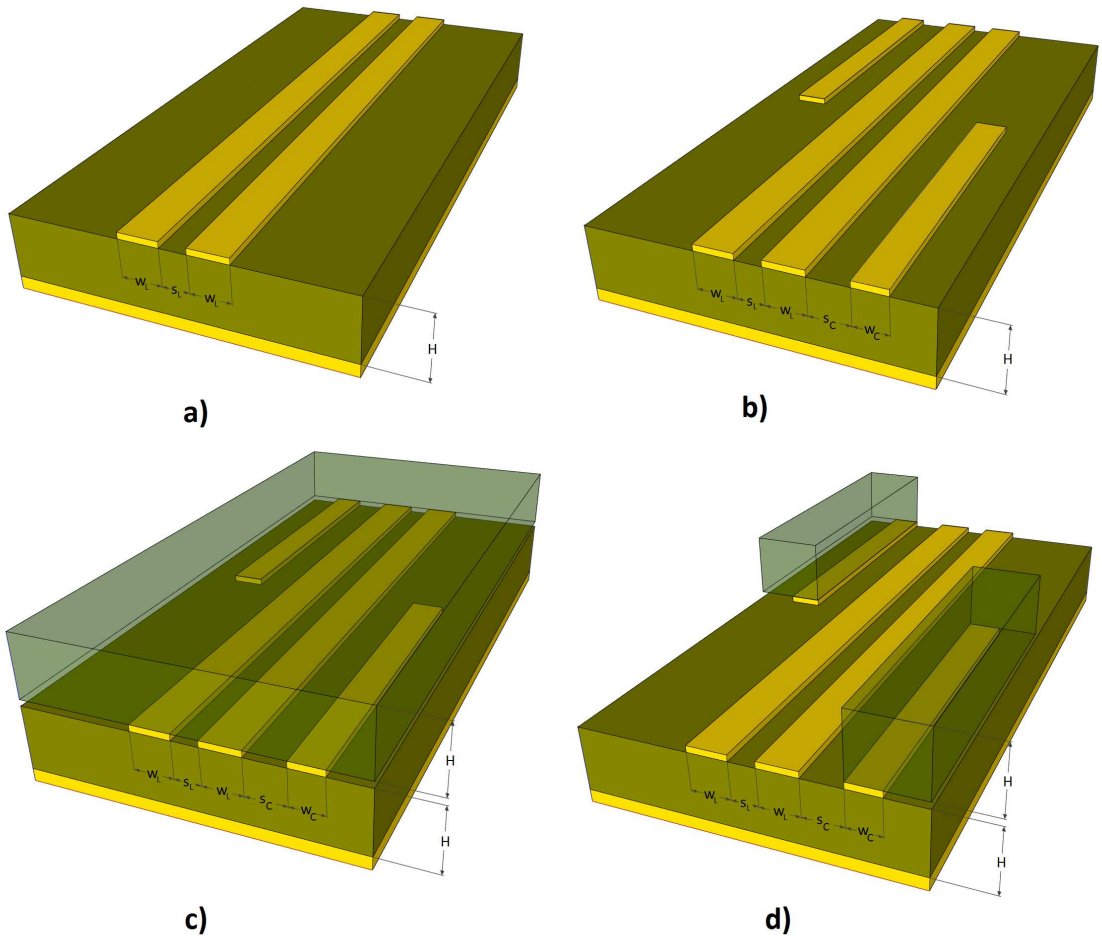

Fig.3 Differential signal coupler topologies: a) differential transmission line, b) differential transmission line with the coupler realized on the same board, c) differential transmission line with the coupler realized on the overlayed board, d) differential transmission line with the coupler realized on the two separate boards overlayed on the board containing the transmission line.

$$C_{ga} = \epsilon_0 \frac{K(k')}{K(k)} \tag{22}$$

$$\frac{K(k')}{K(k)} = \begin{cases} \frac{1}{\pi} ln\left[2\frac{1+\sqrt{k'}}{1-\sqrt{k'}}\right] & \text{for } 0 \leqslant k^2 \leqslant 0.5 \\ \frac{\pi}{ln\left[2\frac{1+\sqrt{k'}}{1-\sqrt{k'}}\right]} & \text{for } 0.5 \leqslant k^2 \leqslant 1 \end{cases} \tag{23}$$

$$k = \frac{\left(\frac{s}{h}\right)}{\left(\frac{s}{h}\right) + \left(\frac{2w}{h}\right)} \tag{24}$$

$$k' = \sqrt{1 - k^2} \tag{25}$$

$$C_{gd} = \frac{\epsilon_0 \epsilon_r}{\pi} ln(P) + 0.65 C_f R \tag{26}$$

$$P = coth\left(\frac{\pi}{4}\frac{s}{h}\right) \tag{27}$$

$$R = \frac{0.02}{\left(\frac{s}{h}\right)}\sqrt{\epsilon_r} + \left(1 - \frac{1}{\epsilon_r^2}\right) \tag{28}$$

The relationship between C_e, C_{e1} and C_o, C_{o1} can be described by the following equations:

$$C_{e1} = \frac{1}{c^2 C_e Z_{oe}^2} \tag{29}$$

$$C_{o1} = \frac{1}{c^2 C_o Z_{oo}^2} \tag{30}$$

where c is a speed of light.

The presented design methodology is suitable for the coupler configuration shown in Fig.3b. Implementation of the coupler shown in Fig.3c results in distortion of the monitored transmission line impedance (ϵ_{eff} for the main transmission line for the coupler section is modified). We expect that the relations described above can also be used for the differential signal coupler design in the topology shown on Fig.3d. This configuration, from the EM point of view, fits to the case when the coupler is realized on the same board as the transmission line, with maintaining feasibility (coupler can be realized on two boards - each branch separately). The next section contains results of practical measurements for the structures in Fig.3 a), b), c) and d).

IV. MEASUREMENTS

In order to demonstrate the validity of the proposed approach, the example transmission line was realized and measured in three different variants. As a target for the practical case of the coupler project, a 142mm-long transmission line allocated on a FR-4 substrate ($\epsilon_r = 4.4$, $h =$ 1.55 mm, copper with thickness - 35 um) was taken (Z_0 = 50 Ω, C_L = -15 dB, w_L = 2.88 mm, s_L = 0.67 mm). The operating frequency f_0 is 1 GHz. A desired coupling factor defined for a single transmission line strip and a coupler branch is -20 dB (this value was taken as a compromise between the two conditions: $C_L > -20dB$ and the probed signal amplification of 20dB for further signal processing is feasible). For this target, the following coupler dimensions were determined: w_C = 3.0192 mm, s_C = 1.5914 mm, L_C = 41.33 mm. The system was measured by the vector network analyzer (Agilent Technologies E5071C) in the frequency band 50 MHz - 4 GHz. To connect the test system with the network analyzer, the SMA connectors were used. Due to the large dimensions of the SMA connectors in comparison to the transmission line widths and spacings, it was necessary to use an additional 50 Ω bent at an angle of 45° lines, which allows us to connect the SMA connectors to the measured transmission line (Fig.4a and Fig.4b). To take into account these additional 50 Ω lines in the measurements, it was necessary to prepare the calibration system (Fig.4c). Calibration of the vector network analyzer with our calibration kit causes that the measurement plane is shifted from the SMA connectors to the K plane (Fig.4a and Fig.4b). The measurements were carried out for the three versions of the differential coupler configurations: a coupler implemented on the same printed board as the monitored transmission line (Fig.3b), a coupler implemented on the separate board which is overlayed on the transmission line's board (Fig.3c), and a coupler implemented on the two separate boards (Fig.3d). Recall that the main purpose for the differential signal coupler design is to deliver a decoupled signal to the subsequent blocks of the measurement system, and the coupler should not disturb the transmission conditions of the monitored line. For that reason all the measurements of the transmission line with the coupler are compared to the reference, which is obtained by measuring the monitored transmission line without a coupler (Fig.3a). The measurement results are shown in Fig.5. We can observe that for the configurations presented in Fig.3b and Fig.3d, the coupler does not substantially affect the match of the main transmission line. The error defined as the difference between the stand-alone transmission line match characteristic and line with the coupler is not grater than 1.5 dB in the frequency band 300 MHz to 1.9 GHz.

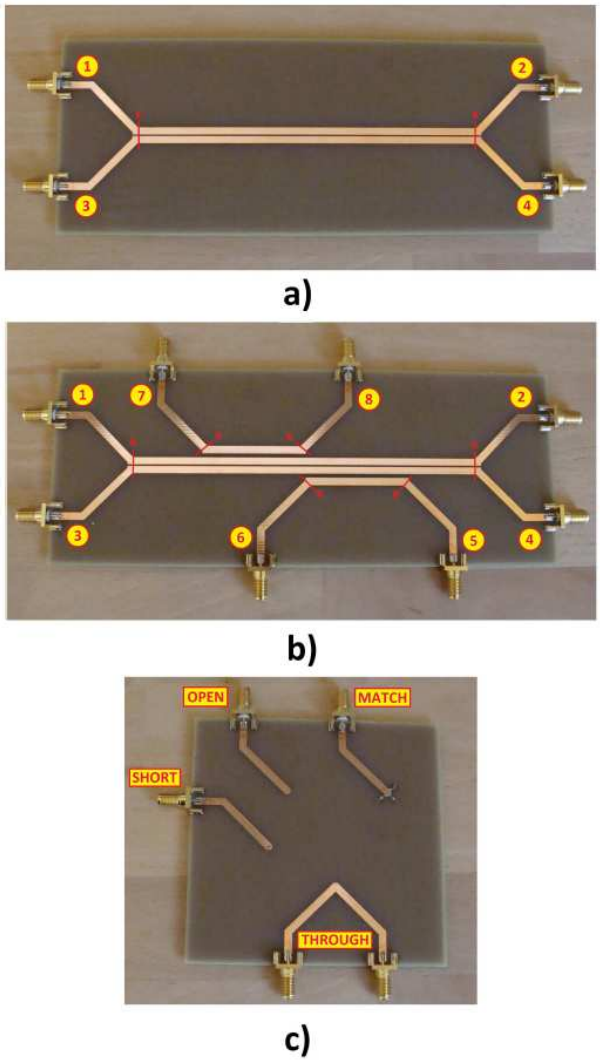

Fig.4 PCBs for measurements: a) reference transmission line, b) transmission line with the differential signal coupler realized on the same board, c) calibration kit.

In these cases, the losses in main transmission line are not changed. The coupling factor for the single coupler's branch at f_0=1 GHz is -19.7 dB. The coupler's branch matching characteristics for the configurations in Figs.3b and 3d are significantly different. This follows from the fact that an additional dielectric layer is overlayed on the coupler's branch in Fig3.d, which modifies the effective dielectric perrmittivity around the branch. The working conditions for the main line in configuration Fig.3c are significantly different from the previous one. The transmission line match is degradated by 9 dB in relation to the configuration without the coupler. Similar observations can be made for the transmission line loss - transmission characteristic strongly deviates from the configuration without the coupler. The branch coupling factor is -17 dB (2.7 dB grater than for other configurations). Such large differences in the measurement results for the configuration in Fig.3c are caused by the additional dielectric overlayed on the measured transmission line. As a result, the effective dielectric permitivity around the transmission line is modified. Hence, the transmission line match, loss characteristic and branch decoupling are

changed. We can observe that for the configurations in Figs.3b and 3d the design goals have been achieved. This confirms the correctness of the proposed design methodology.

It should be noticed that the length of the coupling structure can be reduced by applying numerical optimization of the branch shape. The physical size of the coupler will be also reduced for laminates with higher dielectric constant and for higher resonant frequency f_0 (higher bit rate for main transmission line). These considerations will be the subject of the future work.

V. CONCLUSIONS

In this paper, a new concept of a coupler applicable to high speed data transmission contact-less measurements is presented. A full design methodology of the coupler, with the explicit design formulas is described. The three versions of the differential signal coupler construction were considered. The measurement results for all configurations show that the proposed design methodology is correct and presented concept of coupler (Fig.3d) can be practically used for contact-less monitoring of transmission in high speed interconnections on PCB. The considered contact-less measurement technology allows us to reduce the manufacturing cost of devices, perform debugging process in the late stage of project, and simplify the PCB design process. Future research will include geometry optimization of the coupler in order to broaden the frequency band of operation, improve the branch matching and reduction of length of the coupling structure.

ACKNOWLEDGMENT

The authors would like to thank the company Radmor S.A., Poland, for their help in measuring the fabricated PCB circuit.

REFERENCES

[1] M. Zmuda, S. Szczepański, "A New Approach For High Speed Data Transmission Monitoring", XI International PhD Workshop OWD 2009, 17-20 October 2009

[2] S. Sayil, D. Kerns, S. Kerns, "Comparison of Contactless Measurement and Testing Techniques to a New All-Silicon Optical Test and Characterization Method", IEEE Transactions on Instrumentation and Measurement, Vol. 54, No. 5, October 2005

[3] T. Zelder, B. Geck, M. Wollitzer, I. Rolfes, H. Eul, "Contactless Network Analysis System for the Calibrated Measurement of the Scattering Parameters of Planar Two-Port Device", Proceedings of the 37th European Microwave Conference

[4] T. Zelder, B. Geck, "Contactless Scattering Parameter Measurements", IEEE Microwave and Wireless Components Letters, Vol. 21, No. 9, September 2011

[5] G. Vandersteen, A. Barel, Y. Rolain, "Broadband high frequency differential coupler", Proceedings of the 18th IEEE Instrumentation and Measurement Technology Conference, 2001. IMTC 2001.

[6] A. Eroglu, J. K. Lee, "The Complete Design of Microstrip Directional Couplers Using the Synthesis Method", IEEE Transactions on instrumentation and measurement, Vol. 57, No. 12, December 2008

[7] K. C. Gupta, R. Garg, R. Chadha, "Computer-Aided Design of Microwave Circuits", Artech House INC. 1981

[8] D. M. Pozar, "Microwave Engineering", John Wiley and Sons Inc. 2005

[9] J. Mosenthal, B. Nleya, N. Manthoko,"Broadband / future generation network services deployment in rural and remote areas", ICAST 2009. 2nd International Conference on Adaptive Science and Technology, 2009.

[10] J. Weitzen, T. Grosch, "Comparing coverage quality for femtocell and macrocell broadband data services", IEEE Communications Magazine, January 2010

[11] F. Mekuria, "Enabling wireless broadband technologies and services for the next billion users", AFRICON 2011

[12] J. Koo, K. Chung, "MARC: Adaptive Rate Control scheme for improving the QoE of streaming services in mobile broadband networks", International Symposium on Communications and Information Technologies (ISCIT) 2010

[13] G. Angleou, A. Economides, "Broadband services price competition modeling", 10th Conference of Telecommunication, Media and Internet Techno-Economics (CTTE)

[14] R. Schatz, S. Egger, A. Platzer, "Poor, Good Enough or Even Better? Bridging the Gap between Acceptability and QoE of Mobile Broadband Data Services", 2011 IEEE International Conference on Communications (ICC)

[15] D. Verbitsky, "Early Reliability and Failure Analysis of Cordless Personal Communication Systems", RAMS '07. Annual Reliability and Maintainability Symposium, 2007.

[16] Ch. Tuck-Boon, A. Pant, G. Lerong, P. Gupta, "Design dependent process monitoring for back-end manufacturing cost reduction", IEEE/ACM International Conference on Computer-Aided Design (ICCAD), 2010

[17] C. Berglund, C. Weber, C. Castilla, "An Empirical Study of Photomask Manufacturing Productivity", ASMC 2006. The 17th Annual SEMI/IEEE Advanced Semiconductor Manufacturing Conference, 2006.

[18] R. Andrews, B. Webster, "Managing component variability with a firmware calibration model; reduced manufacturing costs and freedom in vendor selection", Canadian Conference on Electrical and Computer Engineering, 2005.

[19] W. Wei, J. Yang1, T. Ostling, T. Schafer, "New hat feed for reflector antennas realised without dielectrics for reducing manufacturing cost and improving reflection coefficient", IET Microwaves, Antennas and Propagation, 7th December 2010

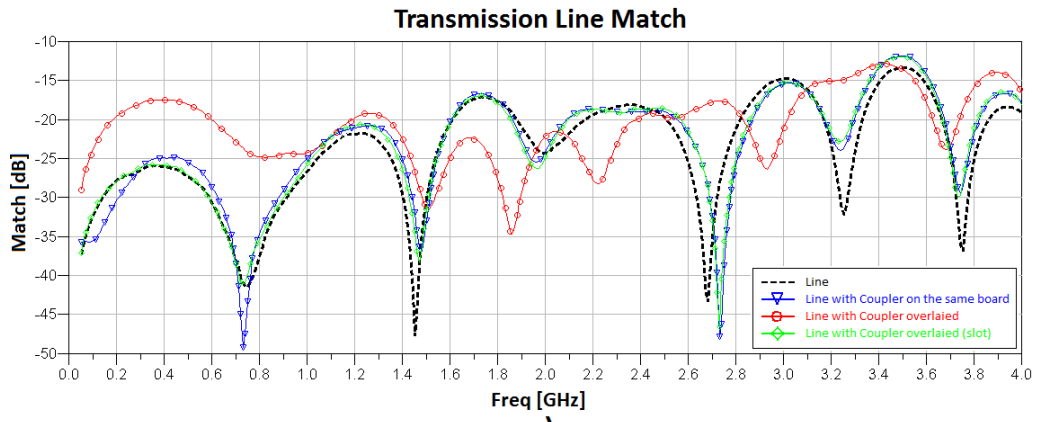

a)

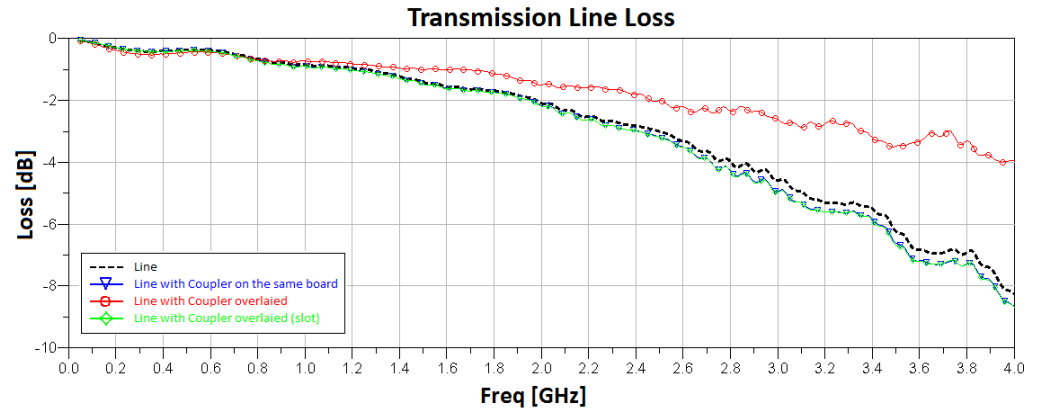

b)

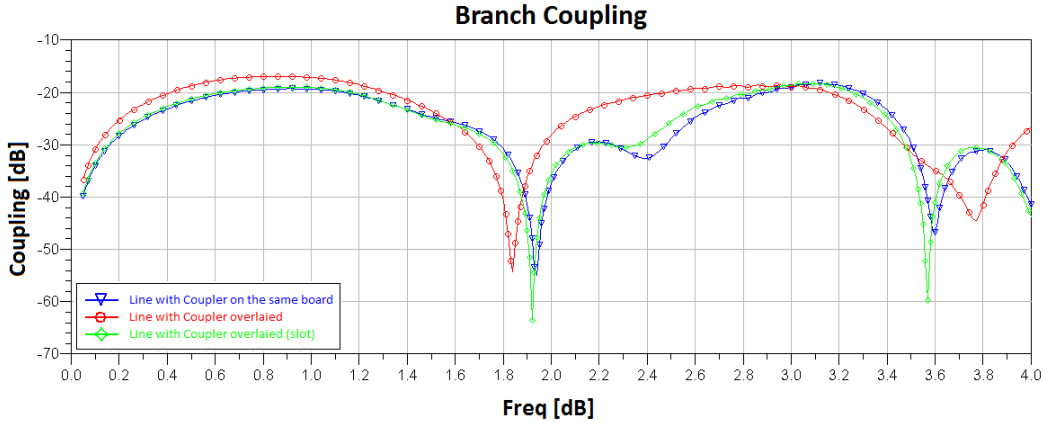

c)

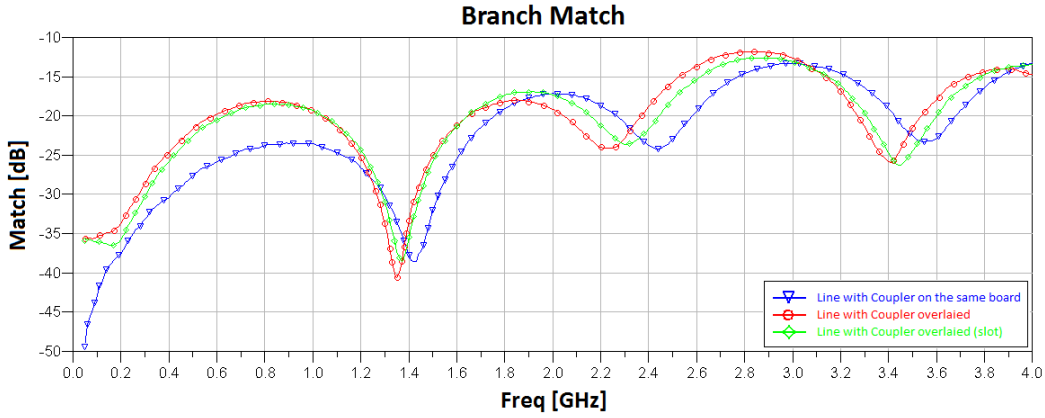

d)

Fig.5 Measurement results

[20] S. Sen, S. Devarakond, A. Chatterjee, "Phase Distortion to Amplitude Conversion-Based Low-Cost Measurement of AM-AM and AM-PM Effects in RF Power Amplifiers", IEEE Transactions on Very Large Scale Integration (VLSI) Systems

[21] A. Ozcelikkale, H. Ozaktas, E. Arikan, "Optimal Measurement under Cost Constraints for Estimation of Propagating Wave Fields", IEEE International Symposium on Information Theory, 2007. ISIT 2007.

[22] Ch. Cheng-Chun, Ch. Chien-Chou, L. Nan-Ting, U. Kurokawa, Ch. Byung, "Spectrum measurement via low cost Spectrum Sensor on-a-chip", Communications and Photonics Conference and Exhibition (ACP), 2010 Asia

[23] S. Sen, S. Devarakond, A. Chatterjee, "Low cost AM/AM and AM/PM distortion measurement using distortion-to-amplitude transformations", International Test Conference, 2009. ITC 2009.

[24] H. Zihong, Ch. Wenhua, Z. Feng, K. Toyama, K. Teshima, "Development of low cost radiated emission measurement system", International Conference on Microwave and Millimeter Wave Technology (ICMMT), 2010

[25] S. Sandeep, A. Vivek, "Design and Development of a Low-Cost Digital Magnetic Field Meter With Wide Dynamic Range for EMC Precompliance Measurements and Other Applications", IEEE Transactions on Instrumentation and Measurement, May 2009